INVESTIGATION OF THE ELASTOPLASTIC BEHAVIOR OF FCC POLYCRYTALS USING A FFT NUMERICAL SCHEME

Abderrahim Belkhabbaz, Brigitte Bacroix, Renald Brenner

INVESTIGATION OF THE ELASTOPLASTIC BEHAVIOR OF FCC POLYCRYTALS USING A FFT NUMERICAL SCHEME

ABDERRAHIM BELKHABBAZ[1], BRIGITTE BACROIX[1], RENALD BRENNER[2]

Abstract. This work is devoted to the study of the effective mechanical response and strain and stress field fluctuations in FCC untextured polycrystals using a full-field numerical approach for a crystalline rate-independent elastoplastic constitutive behavior. The full-field simulations make use of the fast Fourier transform (FFT) numerical scheme. The first application of the developed scheme, which is presented in this paper, is the study of the elastoplastic behavior of non-hardening polycrystals in conjunction with two rate-independent crystal plasticity models: the standard Schmid law and the regularized Schmid law. The macroscopic yield stress is first obtained with the standard Schmid law by averaging the yield stresses calculated on several and different representative volume elements (RVE), each of them being constituted of 500 randomly distributed grains. This numerical estimate is then compared to published results for different nonlinear extensions of the self-consistent (SC) scheme for the case of viscoplasticity at very low rate sensitivity values. Among the different SC models considered, the second-order estimate developed by Ponte Castañeda in 1996 [1] appears to be the most accurate. The influence of the regularization of the Schmid law on the polycrystalline response is then studied using the FFT numerical scheme. It is shown that, unlike the incremental SC model, the FFT numerical estimate is not sensitive to the regularization of the local plastic yield criterion.

Key words: full field modelling, FFT, elasto-plasticity, polycrystalline materials.

1. INTRODUCTION

The homogenization techniques based on mean field approaches are widely used to describe the effective and local properties of polycrystalline aggregates (e.g. [2–5]). This kind of approach provides estimates of the macroscopic mechanical fields based on statistical information on the distributions of the corresponding quantities at the grain level. The self-consistent (SC) model,

[1] CNRS, Laboratoire des Sciences des Procédés et des Matériaux, UPR 3407, Université Paris 13, Sorbonne Paris Cité, F-93430, Villetaneuse, France

[2] Sorbonne Universités, UPMC Université Paris 06, CNRS, UMR 7190, Institut Jean le Rond d'Alembert, F-75005, Paris, France

originally developed by Hershey [6] and Kröner [7] for linear elasticity, is by far the mostly used method for estimating the macroscopic behavior of polycrystalline aggregates. For linear behaviors, this model delivers very accurate estimates for the effective properties as well as for the local strain and stress fields of polycrystalline microstructures [8–11]. This has been assessed by comparisons with full-field numerical results. However, in the case of non-linear behaviors (viscoplasticity for instance), several SC extensions have been proposed leading to very different predictions, especially for highly non-linear behaviors [8, 12, 13]. In order to improve the widely used first-order SC formulations which do not take into account the field fluctuations within the grains, a mean-field approach based on a variational approach has been proposed by Ponte Castañeda [1]. This homogenization scheme, which makes use of the intragranular fluctuations of the fields, delivers estimates that are exact to second-order in the mechanical contrast [14]. It is known as the second-order (SO) method. This method has been later improved by Ponte Castañeda [15, 16]. By comparing various self-consistent estimates to reference full-field calculations, the SO method has been shown to be the most accurate one for isotropic viscoplastic polycrystals [8]. However, until now, no comparison between full-field and mean field approaches has been performed for low rate-sensitivity or rate-independent materials. Such comparisons are thus necessary for the case of rate-independent elasto-plasticity.

At the grain scale, several models can be used for the description of the local rate-independent plasticity criterion. If the standard Schmid law is by far the most widely used, regularized Schmid laws have also been proposed (see, for instance, Gambin [17]). This description is very similar to viscoplastic regularization but remains rate-independent. The crystalline plastic surface is defined by a unique yield function which is differentiable and all the slip systems are active when the plastic criterion is reached. Recently, Yoshida *et al*. [18] studied the influence of the regularization on the incremental self-consistent estimates [19, 20]. By incorporating both standard and regularized Schmid laws into the SC model, they showed that the local strain heterogeneity strongly depends upon the choice of the local constitutive law: the use of regularized Schmid law has been shown to predict much less heterogeneity within the local strain field and a stiffer overall response than the use of the standard Schmid law. Using the regularized law, the incremental SC estimate was found to be very close to the Taylor upper bound. These results have thus highlighted the fact the self-consistent model was significantly affected by the description of the local yield criterion. This is an important shortcoming for this type of approach, as long as more predictive models are searched for.

These differences obtained with the incremental self-consistent scheme, together with the increasing availability of powerful full-field numerical simulations would thus plead in favor of the use of these full-field approaches. And indeed, the classical finite element method (FEM) has been commonly applied to obtain reference solutions for relatively large unit cells or so-called representative volume elements RVE [21–23]. However, the difficulties related to meshing as

well as the large number of degrees of freedom required by such FEM calculations limit the complexity and the size of the microstructures that can be investigated by these methods. In recent years, the drastic increase in computational power has also allowed the development of even more advanced full-field simulations of polycrystalline aggregates. In this context, a novel formulation, originally proposed by Moulinec and Suquet [24] and based on the Fast Fourier Transform FFT technique has been used to overcome the difficulty related to meshing. The latter has been shown to be well adapted to the treatment of composite materials, in which the main source of heterogeneity is related to the spatial distribution of different phases associated with different mechanical properties [25]. Full-field simulations provide, by definition, a numerical estimate of the local stress and strain fields at each voxel. From these local quantities, it is of course possible in turn to calculate statistical averages and fluctuations of stress and strain fields within the individual grains of a polycrystal.

The aim of the present paper is thus to extend the FFT approach to the case of elasto-plasticity for polycrystalline materials. Especially, the influence of the chosen local plasticity criterion will be investigated, in order to see whether this numerical approach is affected or not by this choice (like the SC scheme). The macroscopic FFT estimates will then be compared to SC elastoplastic estimates in order to see whether or not this new approach provides a significantly different response from the one obtained with mean field approaches.

The outline of the present paper is as follows: The main ingredients of the FFT numerical scheme proposed by Moulinec and Suquet [24] are first briefly recalled in Section 2 and the two selected rate independent crystal plasticity laws, i.e. the standard and regularized Schmid laws, are then presented in Section 3. The implementation of the first one is then tested in Section 4, in which the calculation of the tensile yield stress of a FCC isotropic polycristal is presented and compared to self-consistent estimates. The influence of the discretization of the investigated volume and selected number of grains is also discussed. In section 5, the influence of the regularisation of the Schmid law on the elastoplastic behavior is finally analyzed, both in terms of effective behavior and local stress and strain fields.

2. FFT MODELLING

Moulinec and Suquet and Michel et al. [24–26] have developed an iterative method for studying the effective properties and the local field fluctuations within elastoplastic composite materials. It has been further extended to 3D viscoplastic polycrystalline aggregates by Lebensohn [27]. This method allows to obtain a very detailed mapping of the intragranular mechanical fields that appear in a large polycrystalline RVE, in a very efficient way compared with a classical FEM calculation. As no meshing is required, this formulation is particularly adapted to the direct use of images describing the microstructure of the material, obtained either from numerical treatments (like the elaboration of so-called Voronoï

aggregates [10], see below) or experimental measurements [28] (e.g. series of 2D Electron Back Scattering Diffraction (EBSD) files obtained in a scanning electron microscope in order to get a 3D microstructure or direct 3D Diffraction Contrast Tomography (DCT) files obtained in a synchrotron, like that determined by Ludwig et al. [29], Maire et al. [30] or Salvo et al. [31]). Based on such a complete and discrete description of the microstructure, the stress and strains fields can then be computed for each considered voxel. The FFT method is based on the resolution of a unit-cell problem with periodic boundary conditions. The unit cell under consideration is discretized into $N_V = N_x \times N_y \times N_z$ voxels (in three dimensions). We recall that the FFT based algorithm is not restricted to linear behaviors. Problems involving non-linear behaviours like viscoplastic polycrystals [8, 27, 28] and elasto-viscoplastic polycrystals [32, 33] have already been considered.

In the present case which concerns elasto-plasticity, we confine our work to small strains conditions, and we can thus consider the additive decomposition of the local strain rate into elastic and plastic parts

$$\dot{\boldsymbol{\varepsilon}} = \dot{\boldsymbol{\varepsilon}}^e + \dot{\boldsymbol{\varepsilon}}^p . \tag{1}$$

The elastic relation is then given by the Hooke's law

$$\dot{\boldsymbol{\sigma}} = \mathbf{C}^e : \dot{\boldsymbol{\varepsilon}}^e = \mathbf{C}^e : (\dot{\boldsymbol{\varepsilon}} - \dot{\boldsymbol{\varepsilon}}^p) , \tag{2}$$

where $\boldsymbol{\sigma}$ and $\mathbf{C}^e$ are the local true stress and forth-order elastic moduli tensor, respectively. As we deal here with FCC (face-centered cubic) metals, the moduli tensor is characterized by the cubic symmetry and thus contains only 3 distinct elastic constants, namely C_{11}, C_{12} and C_{44}, using the standard Voigt notation. The elastic anisotropy can thus be characterized by the so-called Zener parameter, which reads

$$a = \frac{2C_{44}}{C_{11} - C_{12}} . \tag{3}$$

The local problem on the unit cell with volume Ω and boundary $\partial\Omega$ then reads

$$\begin{cases} \dot{\boldsymbol{\sigma}}(x,t) = \mathbf{C}^e : (\dot{\boldsymbol{\varepsilon}} - \dot{\boldsymbol{\varepsilon}}^p) \quad (x,t) \in \Omega \times [0,T] \\ \operatorname{div} \boldsymbol{\sigma}(x,t) = 0 \\ \boldsymbol{\varepsilon}(x,t) = \operatorname{sym}\left[\operatorname{grad}\left(\mathbf{u}(x,t) \right) \right], \quad \langle \dot{\boldsymbol{\varepsilon}}(x,t) \rangle = \dot{\bar{\boldsymbol{\varepsilon}}}(x,t), \\ \mathbf{u}(x,t) - \langle \boldsymbol{\varepsilon}(x,t) \rangle . x \quad \text{periodic on } \partial\Omega \\ \boldsymbol{\sigma}(x,t) . n \quad \text{anti-periodic on } \partial\Omega \end{cases} \tag{4}$$

with $\dot{\bar{\boldsymbol{\varepsilon}}}(t)$ the imposed macroscopic strain rate and $\boldsymbol{n}$ the outward normal vector on the boundary $\partial\Omega$. The problem is solved incrementally with the integration of the

local constitutive relation. For a given time step t_n, the strain field solution reads

$$\boldsymbol{\varepsilon}(x,t_n) = \overline{\boldsymbol{\varepsilon}}(t_n) - \boldsymbol{\Gamma}^0 * \left(\boldsymbol{\sigma}(x,t_n) - \mathbf{C}^0 : \boldsymbol{\varepsilon}(x,t_n)\right), \tag{5}$$

with $\mathbf{C}^0$ the elasticity tensor of a homogeneous reference medium and $\boldsymbol{\Gamma}^0$ the corresponding Green operator. This implicit integral equation is solved iteratively by using the fixed point method [24]. The plastic flow rule remains to be specified.

3. THE RATE INDEPENDENT CRYSTAL PLASTICITY MODELS

Plastic deformation is supposed to be accommodated by crystallographic slip, which implies that the plastic strain rate takes the form

$$\dot{\boldsymbol{\varepsilon}}^p = \sum_s \dot{\gamma}^{(s)} \mathbf{p}^{(s)} \tag{6}$$

with

$$\mathbf{p}^{(s)} = \frac{1}{2}\left(\mathbf{n}^{(s)} \otimes \mathbf{m}^{(s)} + \mathbf{m}^{(s)} \otimes \mathbf{n}^{(s)}\right), \tag{7}$$

where $\dot{\gamma}^{(s)}$, $\mathbf{n}^{(s)}$ and $\mathbf{m}^{(s)}$ are the slip rate, the slip direction and the slip plane normal for the slip system *(s)*, respectively. For FCC materials, the possible slip systems are the 12 {111} <110> systems (with {111} and <110> the Miller indices of the slip planes and direction families respectively). The resolved shear stress $\tau^{(s)}$ on each system (*s*) is written as

$$\tau^{(s)} = \mathbf{m}^{(s)}.\boldsymbol{\sigma}.\mathbf{n}^{(s)} = \boldsymbol{\sigma} : \mathbf{p}^{(s)}. \tag{8}$$

From Eqs. (2), (6) and (8), the resolved shear stress rate is given as

$$\dot{\tau}^{(s)} = \mathbf{p}^{(s)} : \mathbf{C}^e : \dot{\boldsymbol{\varepsilon}} - \sum_l \dot{\gamma}^{(l)} \mathbf{p}^{(s)} : \mathbf{C}^e : \mathbf{p}^{(l)}, \tag{9}$$

where $\mathbf{p}^{(s)}$ is assumed to be constant. Slip resistance for system (*s*) is denoted by $\tau_c^{(s)}$ (the so-called critical resolved shear stress, CRSS) and its evolution is governed by

$$\dot{\tau}_c^{(s)} = \sum_l h^{sl} \left|\dot{\gamma}^{(l)}\right|, \tag{10}$$

where h^{sl} denotes the so-called hardening matrix, whose actual expression characterizes the selected crystal hardening law.

3.1. THE STANDARD SCHMID LAW (SSL)

For a crystal-plasticity model based on the standard Schmid law (SSL), the local yield function f can simply be written as

$$f = \sup_{s=1,....,N^s} f^{(s)}, \tag{11}$$

with

$$f^{(s)} = \left| \tau^{(s)} \right| - \tau_c^{(s)} = 0. \tag{12}$$

N^s represents the number of slip systems and $f^{(s)}$ describes the yield function for each slip system (s). The plastic strain rate (Eq. (6)) can be re-written as

$$\dot{\boldsymbol{\varepsilon}}^p = \sum_s \operatorname{sgn}\left(\tau^{(s)}\right) \dot{\gamma}^{(s)} \mathbf{p}^{(s)}, \tag{13}$$

where the slip rates are now assumed to be positive.

Based on N^s independent yield functions (Eq. (12)), potentially active and inactive slip systems are then classified as

$$\dot{\gamma}^{(s)} \geq 0 \quad \text{for } f^{(s)} = 0 \text{ and } \dot{f}^{(s)} = 0, \tag{14a}$$

$$\dot{\gamma}^{(s)} = 0 \quad \text{for } f^{(s)} < 0 \text{ and } \dot{f}^{(s)} < 0. \tag{14b}$$

From the consistency condition of the yield functions, the slip rates $\dot{\gamma}^{(s)}$ on the active slip systems are determined from

$$\dot{f}^{(s)} = R^{(s)} - \sum_l X^{sl} \dot{\gamma}^{(l)} = 0, \tag{15}$$

$$\dot{\gamma}^{(s)} = \sum_l Y^{sl} R^{(l)}, \tag{16}$$

with

$$R^{(s)} := \operatorname{sgn}\left(\tau^{(s)}\right) \mathbf{p}^{(s)} : \mathbf{C}^e : \dot{\boldsymbol{\varepsilon}}, \tag{17a}$$

$$X^{(sl)} := h^{(sl)} + \operatorname{sgn}\left(\tau^{(s)}\right) \operatorname{sgn}\left(\tau^{(l)}\right) \mathbf{p}^{(s)} : \mathbf{C}^e : \mathbf{p}^{(l)}, \tag{17b}$$

$$\left[Y^{(sl)}\right] := \left[X^{(sl)}\right]^{-1}. \tag{17c}$$

Under a particular hardening rule, $h^{(sl)}$ and $X^{(sl)}$ may become singular, and this results in a possible non-uniqueness of the set of the active slip systems for a given

deformation mode. But for perfect plasticity ($h^{(sl)} = 0$), it is always possible to choose at least one set of linearly independent slip systems from the potentially active slip systems such that $X^{(sl)}$ is non-singular and Eqs. (15) and (16) are satisfied [19]. If more than five systems are linearly independent, five slip systems are then selected arbitrarily in the computation, a selection mode which has been shown to have a negligible effect on the actual response of the material [18].

Using Eqs. (2), (13) and (16), we finally obtain the rate form of the constitutive equation, $\dot{\boldsymbol{\sigma}} = \mathbf{L} : \dot{\boldsymbol{\varepsilon}}$ in term of the elastoplastic tangent modulus, which writes

$$\mathbf{L} := \mathbf{C}^e - \sum_s \left\{ \left[\operatorname{sgn}\left(\tau^{(s)}\right) \mathbf{C}^e : \mathbf{p}^{(s)} \right] \otimes \sum_l \left[\operatorname{sgn}\left(\tau^{(l)}\right) Y^{(sl)} \right] \mathbf{p}^{(l)} : \mathbf{C}^e \right\}. \quad (18)$$

3.2. THE REGULARISED SCHMID LAW (RSL)

In order to avoid the possible singularity of the matrix $X^{(sl)}$ mentioned above, a regularized Schmid law for rate-independent crystal plasticity has been proposed [17], which can be expressed as

$$f = \left\{ \sum_s \left(\frac{\tau^{(s)}}{\tau_c^{(s)}} \right)^{2n} \right\}^{\frac{1}{2n}} - 1 = 0. \quad (19)$$

In this equation, the exponent n is a material parameter which characterizes in a sense the difference between the normal and the regularized Schmid laws. The plastic strain (Eq. 7) can be derived from the normality rule associated with the yield function given by

$$\dot{\boldsymbol{\varepsilon}}^p = \dot{\Lambda} \frac{\partial f}{\partial \boldsymbol{\sigma}}. \quad (20)$$

By combining Eqs. (6) and (20), the slip rate on a given slip system reads

$$\dot{\gamma}^{(s)} = \frac{\dot{\lambda}}{\tau_c^{(s)}} \left(\frac{\tau^{(s)}}{\tau_c^{(s)}} \right)^{2n-1}, \quad \text{with } \dot{\lambda} = \dot{\Lambda} \left\{ \sum_s \left(\frac{\tau^{(s)}}{\tau_c^{(s)}} \right)^{2n} \right\}^{\frac{1}{2n}-1}, \quad (21)$$

where $\dot{\lambda}$ is a positive plastic multiplier. By contrast to the SSL, all slip rates are derived from a unique plastic multiplier. Therefore, there is no need to classify active and inactive slip systems among the set of slip systems. Loading and unloading conditions are simply written as

$$\dot{\lambda} \geq 0 \quad \text{for } f = 0 \text{ and } \dot{f} = 0, \tag{22a}$$

$$\dot{\lambda} = 0 \quad \text{for } f < 0 \text{ and } \dot{f} \leq 0. \tag{22b}$$

From the consistency condition of the yield function, the plastic multiplier $\dot{\lambda}$ can be determined from

$$\dot{f} = \mathbf{G} : \mathbf{C}^e : \dot{\boldsymbol{\varepsilon}} - \dot{\lambda}(\mathbf{G} : \mathbf{C}^e : \mathbf{G} + H) = 0 \tag{23}$$

and

$$\dot{\lambda} = \frac{\mathbf{G} : \mathbf{C}^e : \dot{\boldsymbol{\varepsilon}}}{\mathbf{G} : \mathbf{C}^e : \mathbf{G} + H}, \tag{24}$$

with

$$\mathbf{G} := \sum_s \left\{ \left(\frac{\tau^{(s)}}{\tau_c^{(s)}} \right)^{2n} \frac{\mathbf{p}^{(s)}}{\tau_c^{(s)}} \right\}, \tag{25a}$$

$$\mathbf{H} := \sum_s \left\{ \left(\frac{\tau^{(s)}}{\tau_c^{(s)}} \right)^{2n} \frac{1}{\tau_c^{(s)}} \sum_l \left[\frac{h^{(sl)}}{\tau_c^{(l)}} \left(\frac{\left| \tau^{(l)} \right|}{\tau_c^{(l)}} \right)^{2n-1} \right] \right\}. \tag{25b}$$

It is worth noting that in this case, no matrix inversion is necessary to get $\dot{\lambda}$. Thus, the difficulty related to the choice of slip systems encountered with the SSL is completely avoided. The elastoplastic tangent modulus reads then

$$\mathbf{L} := \mathbf{C}^e - \frac{(\mathbf{C}^e : \mathbf{G}) \otimes (\mathbf{G} : \mathbf{C}^e)}{\mathbf{G} : \mathbf{C}^e : \mathbf{G} + H}. \tag{26}$$

For the numerical applications presented below, we will restrict ourselves to the case of perfect plasticity, i.e $h^{(sl)} = 0$ and simulate the behavior of copper. Thus, the elastic constants are taken equal to C_{11} = 166 GPa, C_{12} = 120 GPa and C_{44} = 76 GPa, which gives a Zener parameter a = 3.30 and the initial value of the CRSS for all 12 systems is equal to $\tau_c^{(s)} = \tau_c = 30$ MPa. Due to the absence of hardening, this value will remain constant with strain.

4. THE YIELD STRESS OF AN UNTEXTURED FCC POLYCRYSTAL DEFORMED IN UNIAXIAL TENSION

4.1. THE UNIT CELL CONSTRUCTION

As this section is focused on the determination of the yield stress of an isotropic FCC polycrystal using FFT numerical simulations, we first need to construct some isotropic polycrystalline aggregates. Unless otherwise specified, our standard aggregate will be represented by M_g = 500 grains or crystalline phases. Then, to construct a unit cell representative of this aggregate, the so-called Poisson-Voronoï tesselation technique is employed: in this procedure, a set of M_g initial seeds, randomly distributed within the 3D unit cell, is used to generate the tessellation of the whole space. This Poisson distribution of points indeed constitutes the nuclei of the growing grains. Each point within the 3D cell is then assigned to its nearest nucleus determining thus M_g different domains or phases (or grains). Each domain is then associated with a single crystalline orientation extracted from a list of triplets of Euler angles (ϕ_1,Φ, ϕ_2) established using a quasi-random Sobol process. It has been previously checked that this set of orientations does lead to an isotropic (ODF) Orientation Distribution Function. Consequently, the so-obtained 3D unit cell, which is shown in Fig. 1, exhibits a global isotropic behavior. In this figure, each color represents a given crystalline orientation.

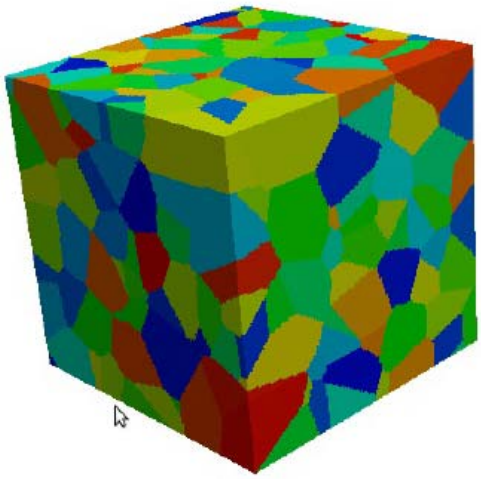

Fig. 1 – An isotropic unit cell containing 500 grains discretized into 200×200×200 voxels (reference microstructure).

This cubic unit cell is then further discretized into a regular grid consisting of $N_V = N_x \times N_y \times N_z$ voxels. By default, we will take $N_x = N_y = N_z = 200$, such that for the standard number of M_g = 500 grains, each grain comprises 16,000 voxels on

average. It is important to note again that periodic boundary conditions will then be imposed to this microstructure to be consistent with the requirements of the FFT-based method. If, in most cases, these periodic conditions are expressed in terms of imposed displacement or strain rate, in some cases, it is necessary to impose instead the stress loading direction [24]. A typical example is provided by the uniaxial tension test along the 3 axis of the sample reference. We impose in this case the direction of the overall stress and we derive the strain loading by means of an auxiliary parameter *t* (arc length method). The overall stress and strain can be expressed as follows:

$$\overline{\sigma} = k S_0 \quad \text{and} \quad \overline{\varepsilon} : S_0 = t \,, \tag{27}$$

where S_0 is the prescribed direction of overall stress, $\overline{\varepsilon}$ is the overall strain, k is the unknown level of overall stress and t, which serves as a loading parameter, is the component of the overall strain in this direction.

4.2. AVERAGING PROCEDURE OVER N DIFFERENT CONFIGURATIONS

In order to assess with accuracy the yield stress of an isotropic polycrystalline material, the constructed unit cell may be too small to constitute a real RVE. In particular, it does not contain several grains associated with the same crystalline orientation but different neighboring environments. In order to overcome this difficulty and to increase the statistical relevance of our calculations, we will calculate the mechanical response of N different unit cells, each of them being associated with the same set of orientations, but with different random distributions of both nuclei positions and associated orientations. By repeating this procedure e.g. 50 times, we end up in this way with 50 different configurations in which the same orientation can be surrounded by different environments. Then, the macroscopic quantities, which will characterize our isotropic polycrystalline material, will simply be obtained by averaging the corresponding quantities calculated for each of the 50 configurations. Taking therefore different grain environments into account by considering different configurations is expected to provide a good approximation of a large isotropic polycrystalline microstructure. In other words, the calculation of the macroscopic yield stress of an isotropic polycrystal will be assessed in the following by performing N calculations on N different unit cells composed of M_g grains and N_V voxels. The larger the parameters N, M_g and N_V, the more precise the mechanical characterization of our isotropic material will be. The use of such averages will then allow us to compare macroscopic and per phase quantities obtained from FFT simulations with analogous quantities obtained from SC formulations for aggregates with random microstructures.

Before doing this comparison, it is first required to perform a preliminary study on the influence of the various parameters which characterize the proposed discretization (number of grid points, orientations and configurations) on the

macroscopic response, in order to determine the set of parameters which provides both satisfactory precision and computing time. For this goal, a tensile test is simulated for several configurations with different Voronoï tessellations and sets of crystalline orientations.

4.3. INFLUENCE OF THE DISCRETIZATION ON THE OVERALL RESPONSE

We start our preliminary study by the evaluation of the influence of the discretization (i.e. the N_V number) on the overall response of the aggregate. The unit cell volume chosen for these simulations contains M_g = 500 grains associated with an isotropic texture and is discretized into $N_V = 8^3$, 16^3, 32^3, 64^3, 100^3 or 200^3 voxels. The evolution of the normalised stress σ_{33}/τ_c as a function of the imposed macroscopic strain $\bar{\varepsilon}$ obtained for these different discretizations in uniaxial tension is shown in Fig.2a. Note that these simulations are performed with a deformation increment $\Delta\bar{\varepsilon} = 5 \cdot 10^{-6}$. We choose here to impose very small increments and thus to reduce the performed calculations to small strains, because we first concentrate on the correction prediction of the elasto-plastic transition. We observe that for a discretization of at least 32^3 voxels, all responses are practically superimposed. The absolute error calculated between the responses obtained using the different discretizations and the one obtained for the extreme case of 200^3 voxels (that we will consider as the reference case for the FFT calculations) is also calculated and presented in Fig. 2b as a function of the imposed deformation. These curves show that the error calculated with a discretization of 32^3 voxels compared to the extreme case of 200^3 voxels is already less than 0.1%, i.e. extremely low. We can thus conclude that the 32^3 discretization can satisfactorily allow the assessment of the macroscopic stress within a reasonable calculation time. This corresponds to a number of voxels per grain η = 65, which seems also quite reasonable, and that we will keep constant in all subsequent calculations. The volume of the RVE is then characterized by the number of grains M_g.

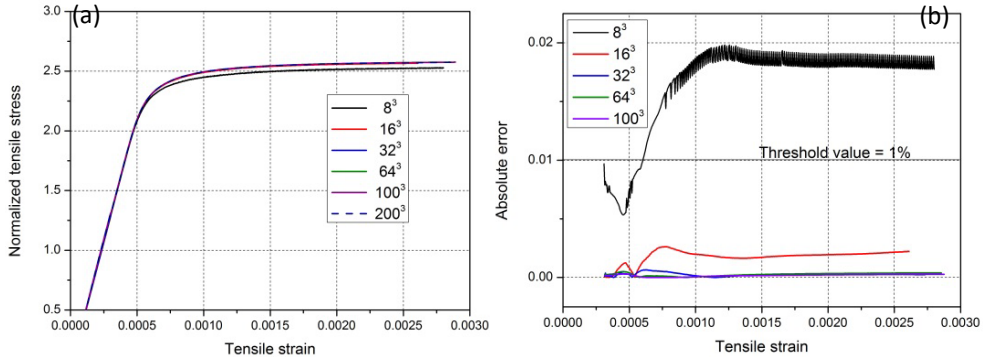

Fig. 2 – a) Macroscopic response for an isotropic FCC polycrystalline aggregate deformed in uniaxial tension using different numbers of voxels N_V; b) evolution with strain of the absolute error between the reference case and the various investigated discretizations.

4.4. INFLUENCE OF THE NUMBER OF GRAINS ON THE OVERALL RESPONSE

We now focus on the influence of the number of grains composing the aggregate on the value the estimated macroscopic yield stress. The definition of the RVE plays a central role in the quality of the prediction of the effective properties of isotropic and heterogeneous materials. Usually, it is simply said that the volume must be large enough with respect to the characteristic length of heterogeneity, but must at the same time involve acceptable computation times. Indeed, the consideration of too large meshes leads to so heavy calculations, that the description of the single crystal constitutive law is often oversimplified in order to compensate the size effect. This is why different studies in the literature have proposed to calculate the effective response for intermediate size volumes [34]. This methodology has, e.g., been applied to characterize the macroscopic elastic behavior [10] or the viscoplastic response of 3D polycrystalline aggregates [8].

In the present work, as we increase the statistical relevance by repeating N times the calculation associated with a unit cell composed of a given number of grains M_g (associated with an imposed number $\eta = 65$ of voxels per grain), we expect that if M_g is increased, we will be able to reduce the number of realizations N to obtain a satisfactory precision. Indeed, for a searched macroscopic property Z, we can evaluate the so-called average $\overline{Z}$ and variance D as follows

$$\overline{Z} = \overline{Z(N, M_g)} = \frac{1}{N}\sum_{i=1}^{N} Z_i(M_g) \tag{28}$$

and

$$D_Z^2 = D(N, M_g)_Z^2 = \frac{1}{N}\sum_{i=1}^{N}\left(\overline{Z} - Z_i(M_g)\right)^2 . \tag{29}$$

Then, we can estimate the so-called relative sampling error on the mean value as [34]

$$\varepsilon_{\text{rel}} = \frac{2D_Z(N, M_g)}{\overline{Z(N, M_g)}\sqrt{N}} = \frac{2D_Z}{\overline{Z}\sqrt{N}} . \tag{30}$$

We thus expect that, if our unit cell is a RVE, the dispersion on the N calculations must be very low, and consequently, the relative sampling error as well. To quantify the accuracy of the full-field results at the global scale, the relative sampling error on the yield stress has thus been calculated for various numbers of configurations N and various numbers of grains M_g. As already mentioned, the number of voxels per grain is fixed to 65, and thus the various numbers of voxels N_V associated with the various considered M_g numbers are listed in Table 1.

Table 1

Selected numbers of grains, voxels and configurations associated with a constant number of voxels per grain ($\eta = 65$) and a relative sampling error equal to 0.7%

Volume of the unit cell = number of grains M_g	Numbers of voxels N_V within the unit cell in order to get $\eta = 65$	Number of configurations N in order to get $\varepsilon_{rel} = 0.7\%$
100	19^3	1100
250	26^3	150
500	32^3	55
1000	41^3	25
5000	70^3	14

Figure 3 presents the evolution of the relative sampling error on the tensile yield stress calculated for different numbers of grains and different numbers of configurations. A significant dispersion of the relative sampling error is observed for the smaller volumes (100 and 250 grains), when the number of configurations is also small (i.e. less than 50). As expected, a decrease of the error is obtained by increasing N. It is worth mentioning that the minimum attainable error depends on the local anisotropy, as well as on the discretization (N_V) and the size of the unit cell (M_g). By imposing a threshold value to the sampling error, we can then define the necessary numbers of grains and configurations to reach an acceptable estimation of the searched property. For a selected threshold of 0.7% for the tensile yield stress of an isotropic FCC polycrystal, the associated N and M_g numbers are listed in Table 1. It is worth mentioning that the macroscopic response is thus identical for all these sets of parameters. The macroscopic tensile yield stress calculated at 0.02% strain with the standard Schmid law for all these sets of parameters is found to be equal to 2.58. In the present case, where no hardening is considered, this value also corresponds to a plastic stationary value. To our knowledge, this is the first accurate computation of the Taylor factor for isotropic elastoplastic FCC polycrystals based on full-field computations for Voronoï tesselations.

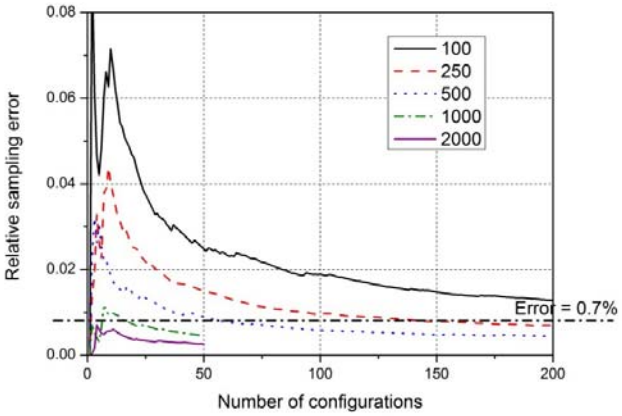

Fig. 3 – Evolution of the sampling error as a function of the number of configurations N for different volumes (defined by the number of grains M_g).

4.5. COMPARISON BETWEEN THE ELASTOPLASTIC FFT PREDICTION AND THE SELF-CONSISTENT ESTIMATES

This elastoplastic FFT estimate of the tensile yield stress of an isotropic FCC aggregate is now compared to the various self-consistent estimates already published for the case of rate-dependent plasticity. These are reported in Fig. 4 in which the evolution of the normalised yield stress of an untextured FCC polycrystal is presented as function of the strain rate sensitivity m for different self-consistent estimates in viscoplacity, including the FFT approach [12, 13]. The rate independent case corresponds to the limit $m = 0$. It is worth mentioning that this estimate is not reported for very low values of m for both FFT and SO approaches (see Fig. 4). This is likely due to convergence issues. It is also obvious that the discrepancy between the various nonlinear viscoplastic SC estimates increases with increasing nonlinearity (i.e. with decreasing m). It is recalled that, for $m = 1$ (linear viscosity), all SC estimates coincide (see Fig. 4).

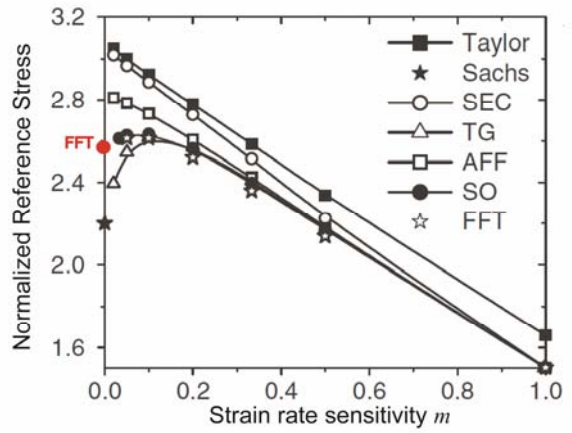

Fig. 4 – Evolution of the normalized reference tensile stress of an FCC isotropic polycrystal with the strain rate sensitivity, calculated with various SC and FTT estimates [13]. In the legend, SEC = secant, TG = tangent, AFF = affine and SO = second order.

More precisely, for low m values, it is seen that the classical incremental SC estimate (i.e. the secant one) tends to the upper bound approach (the Taylor model) and predicts thus a too stiff response. On the other hand, the tangent, second-order and affine estimates, which all rely on a similar linearization scheme, are seen to produce a softer response. It is known that the tangent approach rigorously coincide with the static model (lower bound) for $m = 0$. The affine and second-order estimates are clearly different for high nonlinearity.

Interestingly, it can be noted that, among the different nonlinear extensions of the SC model, the SO method predicts the most accurate value compared to our reference FFT result, when m is close to 0. This result is consistent with previous results for highly anisotropic viscoplastic polycrystals [3, 8].

5. THE INFLUENCE OF THE REGULARIZATION OF THE SCHMID LAW

5.1. THE UNIAXIAL TENSILE STRESS FOR AN UNTEXTURED FCC POLYCRYSTAL

In order to analyze now the influence of the regularization of the Schmid law on the elastoplastic FFT estimate of the polycrystal response, we again simulate a tensile test on the same FFC polycrystal (elastically anisotropic and untextured) as the one used in Section 4. Its microstructure is thus represented by 500 crystalline phases and no hardening is considered. The predicted macroscopic uniaxial stress-strain curve is presented in Fig. 5a for different values of the exponent *n*. The stress is normalized by the critical resolved shear stress of the slip systems (one single and constant value for all systems of all the grains). As expected, the softer response is found for the lowest *n* value and the response obtained with the regularized Schmid law is very close to the one obtained with the standard one for high values of *n* (i.e. larger than 50). We obtain in this case the same value of the yield stress as the one obtained with the standard Schmid law, namely 2.58. It is worth noting that the yield stress obtained with the regularised Schmid law using the elastoplastic FFT model is significantly lower than the value obtained using the incremental secant self-consistent estimate [8]. For the latter case, the yield stress saturates at the value of 3.06, which is the same as the well-known upper bound Taylor value for rigid plastic FCC polycrystals (see Fig. 5b). Thus, in opposition to the SC incremental model, the elastoplastic FFT model is not sensitive to the regularization of the Schmid law, which is indeed a major positive point for this model.

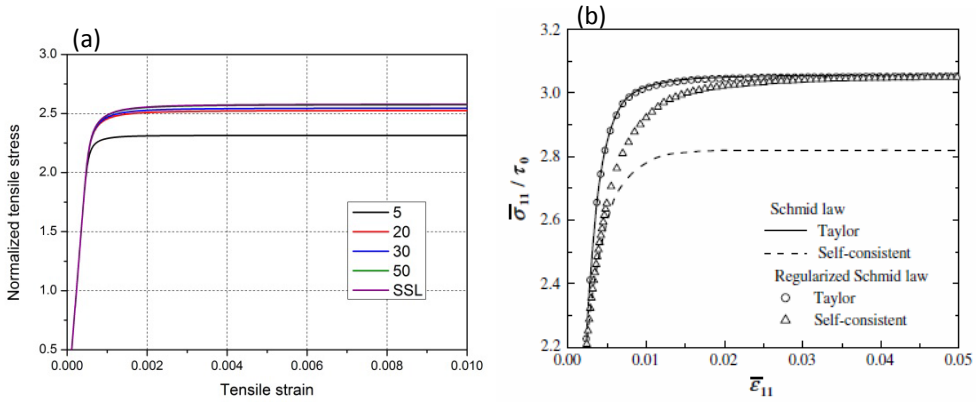

Fig. 5 – Macroscopic uniaxial stress-strain curves for FCC isotropic polycrystals obtained with: a) the elastoplastic FFT model in conjunction with the regularized Schmid law with different *n* exponents; b) the Taylor and SC incremental models [18] with the standard (SSL) and regularized Schmid laws.

5.2 THE LOCAL FIELD FLUCTUATIONS

The attention is now focused on the quantitative comparison of the local field fluctuations during the the elastoplastic transition obtained in tension with the FFT model, using either the standard Schmid law or its regularised version. The exponent of the regularized Schmid law is taken equal to $n = 50$, in order to get very close responses between both Schmid laws. Figure 6 shows the evolution of the local strain component within each of the 500 grains, normalized by the macroscopic tensile strain using respectively the standard Schmid law (left) and the regularised one (right). We can observe that both laws predict the same range of heterogeneity for the deformation field. Especially, after only 0.2% strain, the range of variation of the local ε_{33} strain component is ±64%, and the two calculated strain fields are hardly distinguishable. We can thus conclude that these two descriptions of the crystalline plastic behavior will lead to very close global plasticity criteria and can thus be equally used. This was not the case for the SC model, as shown in ref. [18].

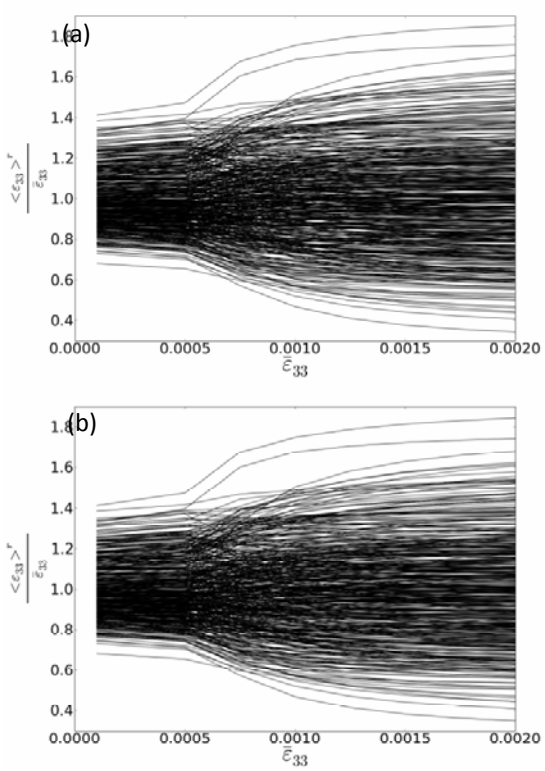

Fig. 6 – Evolution of the local strain within each of the 500 grains as a function of the macroscopic one, using: a) the standard Schmid law; b) the regularized Schmid law.

6. CONCLUSIONS

In this paper, the homogenization technique based on the FFT numerical scheme has been used to calculate estimates of the effective behaviour, as well as of the strain field fluctuations within untextured FFC polycrystals in conjunction with two rate independent crystal plasticity models, namely the standard Schmid law and the regularised Schmid law. The standard Schmid one has been used to characterize the macroscopic yield stress for untextured microstructures. To be more representative, this yield stress has been estimated from the calculation of averages performed on rather small unit cells. Our analysis focused first on the influence of the simulation parameters (numbers of grains, voxels and configurations) on the macroscopic response. This preliminary study showed a relatively weak influence of the voxel number on the macroscopic response, but a significant influence of the number of configurations.

Various self-consistent estimates of the macroscopic response of isotropic FCC aggregates, associated with very low values of the rate sensitivity parameter m, have then been compared to a reference case calculated with the elastoplastic FFT approach (large number of grains and configurations). Among all tested SC estimates, the SO one appears to be the closest to our reference value.

Then, the effect of the regularization of the Schmid law on the macroscopic response has been investigated. It has been shown, that with an appropriate choice of the exponent n, the two Schmid laws provide undistinguishable macroscopic responses as well as local strain fields. This is thus different from what was found for the SC incremental model, which was shown to abnormally depend on the local single crystal plasticity law.

As a general conclusion, the FFT method has been shown to be quite robust in elasto-plasticity and to provide very precise estimates of the global and local response of untextured polycrystals. There remains now to test further this approach on textured and hardening materials.

Acknowledgements. B. Bacroix and R. Brenner gratefully acknowledge the numerous, enthousiastic and fruitful discussions, shared with C. Teodosiu during many years, and especially about physically-based single crystal and polycrystalline constitutive laws; surely, these have enriched their reflection on the relevance of developing advanced models for a better description of the mechanical behavior of polycrystalline materials.

Received on March 28, 2015

REFERENCES

1. CASTAÑEDA, P.P., *Exact second-order estimates for the effective mechanical properties of nonlinear composite materials*, Journal of the Mechanics and Physics of Solids, **44**, *6*, pp. 827–862, 1996.

2. BRENNER, R., BECHADE, J.L., CASTELNAU, O., BACROIX, B., *Thermal creep of Zr-Nb1%-O alloys: experimental analysis and micromechanical modelling*, Journal of Nuclear Materials, **305**, *2–3*, pp. 175–186, 2002.
3. CASTELNAU, O., BLACKMAN, D.K., LEBENSOHN, R.A., CASTAÑEDA, P.P., *Micromechanical modeling of the viscoplastic behavior of olivine*, Journal of Geophysical Research-Solid Earth, **113**, B09202, 2008.
4. BRENNER, R., BECHADE, J.L., CASTELNAU, O., BACROIX, B., *Modelling of the thermal creep of Zircaloy-4 using a self-consistent affine estimate*, in: *Advances in Mechanical Behaviour, Plasticity and Damage*, Vols. 1 and 2 (eds. D. Miannay *et al.*), 2000, pp. 359–364.
5. LEBENSOHN, R.A., TURNER, P.A., SIGNORELLI, J.W., CANOVA, G.R., TOME, C.N., *Calculation of intergranular stresses based on a large-strain viscoplastic self-consistent polycrystal model*, Modelling and Simulation in Materials Science and Engineering, **6**, *4*, pp. 447–465, 1998.
6. HERSHEY, A.V., *The elasticity of an isotropic aggregate of anisotropic cubic crystals*, Journal of Applied Mechanics–Transactions of the ASME, **21**, pp. 236–240, 1954.
7. KRONER, E., *Berechnung der Elastischen Konstanten des Vielkristalls aus den Konstanten des Einkristalls*, Zeitschrift für Physik, **151**, *4*, pp. 504–518, 1958.
8. LEBENSOHN, R.A., LIU, Y., CASTAÑEDA, P.P., *On the accuracy of the self-consistent approximation for polycrystals: comparison with full-field numerical simulations*, Acta Materialia, **52**, *18*, pp. 5347–5361, 2004.
9. CASTELNAU, O., BRENNER, R., LEBENSOHN, R.A., *The effect of strain heterogeneity on the work hardening of polycrystals predicted by mean-field approaches*, Acta Materialia, **54**, *10*, pp. 2745–2756, 2006.
10. BRENNER, R., LEBENSOHN, R.A., CASTELNAU, O., *Elastic anisotropy and yield surface estimates of polycrystals*, International Journal of Solids and Structures, **46**, *16*, pp. 3018–3026, 2009.
11. BELKHABBAZ, A., BRENNER, R., RUPIN, N., BACROIX, B., FONSECA, J., *Prediction of the overall behavior of a 3D microstructure of austenitic steel by using FFT numerical scheme*, Procedia Engineering, **10**, pp. 1883–1888, 2011.
12. BORNERT, M., MASSON, R., CASTAÑEDA, P.P., ZAOUI, A., *Second-order estimates for the effective behaviour of viscoplastic polycrystalline materials*, Journal of the Mechanics and Physics of Solids, **49**, *11*, pp. 2737–2764, 2001.
13. LEBENSOHN, R.A., TOME, C.N., CASTAÑEDA, P.P., *Self-consistent modelling of the mechanical behaviour of viscoplastic polycrystals incorporating intragranular field fluctuations*, Philosophical Magazine, **87**, *28*, pp. 4287–4322, 2007.
14. SUQUET, P., PONTE CASTAÑEDA, P., *Small-contrast perturbation expansions for the effective properties of nonlinear composites*, C. R. Acad. Sci. Paris, **317**, pp. 1515–1522, 1993.
15. PONTE CASTAÑEDA, P., *Second-order homogenization estimates for nonlinear composites incorporating field fluctuations: II–applications*, Journal of the Mechanics and Physics of Solids, **50**, *4*, pp. 759–782, 2002.
16. PONTE CASTAÑEDA, P., *Second-order homogenization estimates for nonlinear composites incorporating field fluctuations: I–theory*, Journal of the Mechanics and Physics of Solids, **50**, *4*, pp. 737–757, 2002.
17. GAMBIN, W., *Refined analysis of elastic-plastic crystals*, International Journal of Solids and Structures, **29**, *16*, pp. 2013–2021, 1992.
18. YOSHIDA, K., BRENNER, R., BACROIX, B., BOUVIER, S., *Effect of regularization of Schmid law on self-consistent estimates for rate-independent plasticity of polycrystals*, European Journal of Mechanics – A/Solids, **28**, *5*, pp. 905-915, 2009.
19. HUTCHINSON, J., *Elastic-plastic behaviour of polycrystalline metals and composites*, Proceedings of the Royal Society of London Series A – Mathematical and Physical Sciences, **319**, pp. 247–256,1970.
20. HILL, R., *A self-consistent mechanics of composite materials*, Journal of the Mechanics and Physics of Solids, **13**, *4*, p. 213–222, 1965.

21. BARBE, F., DECKER, L., JEULIN, D., CAILLETAUD, G., *Intergranular and intragranular behavior of polycrystalline aggregates. Part 1: FE model*, International Journal of Plasticity, **17**, *4*, pp. 513–536, 2001.
22. ZEGHADI, A., FOREST, S., GOURGUES, A.F., BOUAZIZ, O., *Ensemble averaging stress–strain fields in polycrystalline aggregates with a constrained surface microstructure - Part 2: crystal plasticity*, Philosophical Magazine, **87**, *8–9*, pp. 1425–1446, 2007.
23. MUSIENKO, A., TATSCHL, A., SCHMIDEGG, K., KOLEDNIK, O., PIPPAN, R., CAILLETAUD, G., *Three-dimensional finite element simulation of a polycrystalline copper specimen*, Acta Materialia, **55**, *12*, pp. 4121–4136, 2007.
24. MOULINEC, H., SUQUET, P., *A numerical method for computing the overall response of nonlinear composites with complex microstructure*, Computer Methods in Applied Mechanics and Engineering, **157**, *1–2*, pp. 69–94, 1998.
25. MOULINEC, H., SUQUET, P., *Intraphase strain heterogeneity in nonlinear composites: a computational approach*, European Journal of Mechanics – A/Solids, **22**, *5*, pp. 751–770, 2003.
26. MICHEL, J.C., MOULINEC, H., SUQUET, P., *A computational scheme for linear and non-linear composites with arbitrary phase contrast*, International Journal for Numerical Methods in Engineering, **52**, *1–2*, pp. 139–160, 2001.
27. LEBENSOHN, R.A., *N-site modeling of a 3D viscoplastic polycrystal using Fast Fourier Transform*, Acta Materialia, **49**, *14*, pp. 2723–2737, 2001.
28. LEBENSOHN, R.A., BRENNER, R., CASTELNAU, O., ROLLETT, A.D., *Orientation image-based micromechanical modelling of subgrain texture evolution in polycrystalline copper*, Acta Materialia, **56**, *15*, pp. 3914–3926, 2008.
29. LUDWIG, W., SCHMIDT, S., LAURIDSEN, E.M., POULSEN, H.F., *X-ray diffraction contrast tomography: a novel technique for three-dimensional grain mapping of polycrystals. I. Direct beam case*, Journal of Applied Crystallography, **41**, *2*, pp. 302–309, 2008.
30. MAIRE, E., CARMONA, V., COURBON, J., LUDWIG, W., *Fast X-ray tomography and acoustic emission study of damage in metals during continuous tensile tests*, Acta Materialia, **55**, *20*, pp. 6806–6815, 2007.
31. SALVO, L., CLOETENS, P., MAIRE, E., ZABLER, S., BLANDIN, J.J., BUFFIÈRE, J.Y., LUDWIG, W., BOLLER, E., BELLET, D., JOSSEROND, C., *X-ray micro-tomography an attractive characterisation technique in materials science*, Nuclear Instruments and Methods in Physics Research Section B: Beam Interactions with Materials and Atoms, **200**, pp. 273–286, 2003.
32. SUQUET, P., MOULINEC, H., CASTELNAU, O., MONTAGNAT, M., LAHELLEC, N., GRENNERAT, F., DUVAL, P., BRENNER, R., *Multi-scale modeling of the mechanical behavior of polycrystalline ice under transient creep*, Iutam Symposium on Linking Scales in Computations: From Microstructure to Macro-Scale Properties, Vol. 3, pp. 76–90, 2012.
33. GRENNERAT, F., MONTAGNAT, M., CASTELNAU, O., VACHER, P., MOULINEC, H., SUQUET, P., DUVAL, P., *Experimental characterization of the intragranular strain field in columnar ice during transient creep*, Acta Materialia, **60**, *8*, pp. 3655–3666, 2012.
34. KANIT, T., FOREST, S., GALLIET, I., MOUNOURY, V., JEULIN, D., *Determination of the size of the representative volume element for random composites: statistical and numerical approach*, International Journal of Solids and Structures, **40**, *13–14*, pp. 3647–3679, 2003.